

# ANALYTICAL MODEL FOR P-N JUNCTIONS UNDER POINT SOURCE ILLUMINATION

B. Blanco-Filgueira, P. López

Dept. of Electronics and Computer Science  
University of Santiago de Compostela  
15782 Santiago de Compostela, Spain  
Email: beatriz.blanco;p.lopez@usc.es

J. Döge

Fraunhofer Institute for Integrated Circuits  
Design Automation Division  
Zeunerstr. 38, 01069 Dresden, Germany  
Email: Jens.Doege@eas.iis.fraunhofer.de

## ABSTRACT

An analytical model of the photoresponse of p-n junctions under a point source illumination is presented. The model measures the response of different regions of the pixel in terms of current. Both p-n<sup>+</sup> and p-N<sub>well</sub> junction photodiodes were fabricated in a standard UMC 90nm technology and tested. Model and experimental data reveal a similar behaviour.

**Index Terms**— Image sensors, Photodiodes, Modeling.

## 1. INTRODUCTION

Complementary metal-oxide semiconductor (CMOS) image sensors offer interesting advantages over Charge Coupled Device (CCD) technology [1]. However, it is necessary to put effort into a comprehensive study of the main physical phenomena dominating the behaviour of pixels at these technological nodes in order to exploit their advantages.

As CMOS image sensors benefit from technology scaling new challenges arise [2]. To overcome this, not only technological changes in CMOS fabrication processes and alternative pixel architectures need to be investigated But, more importantly, a profound understanding of the physical processes governing the behavior of deep submicron and even nano photodiode structures are necessary to achieve an optimal pixel design.

Previous studies are focused on the experimental characterization and comparison of different pixel cells [3, 4]. Nowadays, this procedure is not cost-effective and it is desirable to have models in order to predict the pixel behaviour. Although there are publications on pixel size and shape [5], and even some semi-analytical models of the pixel photoresponse as a function of the active area size [6, 7], there is a lack of studies at sub-pixel level; that is, about the contribution of the different regions of the pixel. In this paper we present an analytical model for p-n junctions under a point source illumination. Moreover, we show experimental data corresponding to the output current of p-n<sup>+</sup> and p-N<sub>well</sub> junction photodiodes (PD) fabricated in a standard UMC 90nm technology, where the electronics corresponds to a 3T-APS standard architecture.

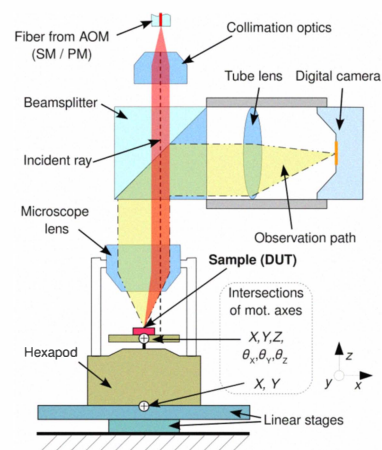


Fig. 1. Scheme of the optical set-up.

In Section 2 the experimental set-up of the measurements is described. The analytical model is explained in Section 3 considering the different regions of the pixel. Finally, the model is compared with experimental data and conclusions are summarized in Section 4.

## 2. EXPERIMENTAL SET-UP

The experimental set-up, Fig. 1, consists of an optical part for illumination and observation of the sample (device under test, DUT) and a mechanical part for its precise positioning.

The DUT is illuminated by a laser beam of variable power generated by a nonlinear photonic-crystal fiber (PCF) laser. Up to 8 different wavelength values can be selected simultaneously by an acousto-optic modulator (AOM). The coupling between AOM and optical set-up is realized through three different exchangeable single mode polarization maintaining (SM/PM) fibers (blue, red, and NIR). The illumination path leads from the fiber to the radiation sensitive DUT via collimation optics, beamsplitter cube, and microscope lens. The surface of the DUT with the projected light spot is observed through the same microscope lens with observation

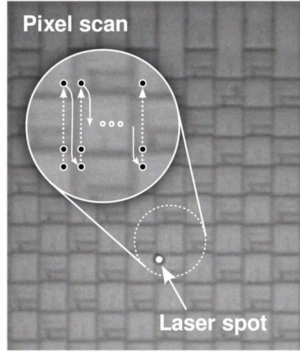


**Fig. 2.** Microphotography of the image sensor matrix with the laser spot and the scanned pixel region with the photodiode.

path through the beamsplitter cube and a tube lens mounted to a digital camera. For the coaxial white-light illumination of the chip-surface, necessary for taking microphotographic pictures as in Fig. 2, a second beamsplitter is used (not depicted in Fig. 1).

The DUT is attached to the platform of the hexapod and can be positioned in 6 axes. The microscope lens is mounted to the body of the hexapod. The whole assembly is moved by two linear stages relative to the beamsplitter, so the angle of the laser illumination can be adjusted.

### 3. ANALYTICAL MODEL

In this work, an analytical expression of the photoresponse of p-n junctions under point source illumination is achieved by solving the continuity equation in the different regions of the pixel. Fig. 3 shows the modelled pixel photosensitive area cross sections. They consist of reverse biased p-n<sup>+</sup> and p-N<sub>well</sub> junction photodiodes (PD) with junction depth  $y_j$  and wafer thickness  $y_w$ . The n<sup>+</sup> diffusion and the device are  $x_{ph}$  and  $x_l$  wide, respectively. Diffusion depth and well width for the p-N<sub>well</sub> junction are  $y_{ph}$  and  $x_{well}$ . In reverse-bias operation three main regions are distinguished in the device: two quasi-neutral regions and the depletion region with thickness  $W$ . We assume the depletion region located in the substrate because diffusion concentration is higher.

The main objective is to model the total current density through these devices under a point source illumination impinging perpendicular onto the top surface. The overall photogenerated current density is given by the sum of the different contributions of the single regions. As the source is smaller than a pixel, the response depending on the illuminated pixel region can be observed. Moreover, the importance of the peripheral contribution to the total photoresponse can be studied. In this way, if the pixel is scanned with a point source as shown in Fig. 2, four different regions can be differentiated: (i) electronics, (ii) active area, (iii) lateral depletion region, and (iv) surroundings.

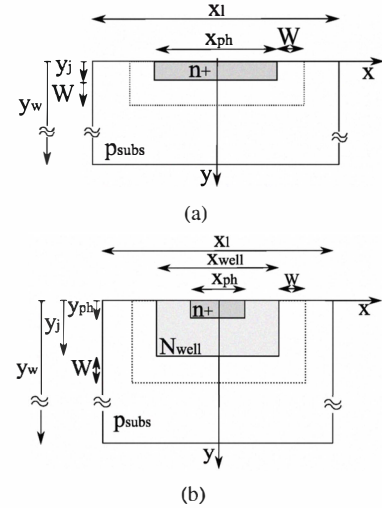


**Fig. 3.** Photodiode structures. a) p-n<sup>+</sup> and b) p-N<sub>well</sub>

In the first case, (i), it is assumed that the response is close to zero because photocarriers are not likely to be generated in the electronics region. Then, the output current is equal to the saturation current of the inversely biased p-n junction  $I_o = q (x_{ph}^2 + 4x_{ph}y_j) \left( \frac{D_n}{L_n} n_{p0} + \frac{D_p}{L_p} p_{n0} \right)$ , where  $x_{ph}^2$  and  $4x_{ph}y_j$  are the bottom and side-wall areas of the junction, respectively. This current is negligible and it will not be considered as from now.

There are previous works that have tackled the calculation of the output current density when the active area is illuminated (ii). In [8] a mathematical model of the photogenerated current density on a n-p<sup>+</sup> junction PD is presented. In our case, proceeding in a similar way, the stationary continuity equation in one dimension is solved in the quasi-neutral regions as the minority carriers mainly move there by diffusion:

$$D_n \frac{\partial^2 (n_p - n_{p0})}{\partial y^2} - \frac{n_p - n_{p0}}{\tau_n} + G(y) = 0 \quad (1)$$

where  $n_p$  and  $n_{p0}$  are the electron concentration and its equilibrium value, respectively,  $D_n$  and  $\tau_n$  are the electron diffusion coefficient and lifetime, and  $G(y) = -\frac{\partial \Phi}{\partial y}$  is the optical generation rate, i.e. the number of photogenerated electron-hole pairs per unit volume and time (where  $\Phi$  is the photon flux). According to the Beer's law,  $\Phi$  decreases exponentially with the depth in Si,  $y$ ,  $\Phi(y) = \Phi_0 e^{-\alpha y}$ , where  $\alpha$  is the absorption coefficient and  $\Phi_0$  is the photon flux at the silicon surface. The latter can be written as  $\Phi_0 = \frac{P_{opt} T}{h\nu}$ , where  $P_{opt}$  represents the incident optical power,  $T$  the transmission coefficient,  $h$  the Plank's constant, and  $\nu$  the impinging radiation frequency. The generic solution of Eq. (1) is:

$$n_p(y) = n_{p0} + \frac{\Phi_0 \alpha \tau_n}{1 - \alpha^2 L_n^2} e^{-\alpha y} + A e^{-y/L_n} + B e^{y/L_n} \quad (2)$$

where  $L_n$  is the electron diffusion length. The procedure is

the same for holes in the  $n^+$  region

$$p_n(y) = p_{n0} + \frac{\Phi_0 \alpha \tau_p}{1 - \alpha^2 L_p^2} e^{-\alpha y} + C e^{-y/L_p} + D e^{y/L_p} \quad (3)$$

Eq. (2) and Eq. (3) are solved subjected to the boundary conditions

$$\begin{aligned} n_p(\infty) &= n_{p0} & n_p(y_j + W) &= n_{p0} e^{qV_{PD}/KT} \\ p_n(0) &= p_{n0} & p_n(y_j) &= p_{n0} e^{qV_{PD}/KT} \end{aligned} \quad (4)$$

to calculate the constants  $A$ ,  $B$ ,  $C$ , and  $D$ , where  $V_{PD}$ ,  $K$ , and  $T$  are the inverse-biased voltage of the photodiode, Boltzmann constant and temperature, respectively. Eq. (3) must be rewritten to distinguish between diffusion and well regions for the p-N<sub>well</sub> :

$$p_n(y) = \begin{cases} p_{n1}(y), & 0 \leq y \leq y_{ph} \\ p_{n2}(y), & y_{ph} \leq y \leq y_j \end{cases} \quad (5)$$

where

$$\begin{aligned} p_{n1}(y) &= p_{n01} + \frac{\Phi_0 \alpha \tau_p}{1 - \alpha^2 L_{p1}^2} e^{-\alpha y} + C_1 e^{-y/L_{p1}} + D_1 e^{y/L_{p1}} \\ p_{n2}(y) &= p_{n02} + \frac{\Phi_0 \alpha \tau_p}{1 - \alpha^2 L_{p2}^2} e^{-\alpha y} + C_2 e^{-y/L_{p2}} + D_2 e^{y/L_{p2}} \end{aligned} \quad (6)$$

The following boundary conditions are used to achieve the solution:

$$\begin{cases} J_p = -qD_{p1} \frac{\partial p_{n1}(y)}{\partial y} \Big|_{y_{ph}} = -qD_{p2} \frac{\partial p_{n2}(y)}{\partial y} \Big|_{y_{ph}} \\ p_{n1}(y_{ph}) = p_{n2}(y_{ph}) \\ p_n(0) = p_{n01} \\ p_n(y_j) = p_{n0} e^{qV_{PD}/KT} \end{cases} \quad (7)$$

So, the spatial distributions of the quasi-neutral region contributions to the current density are

$$J_n(y) = qD_n \frac{\partial n_p(y)}{\partial y} \quad J_p(y) = -qD_p \frac{\partial p_n(y)}{\partial y} \quad (8)$$

In the depletion region carriers mainly move by drift. The high electric field inside this region moves charges out to neutral regions before they can recombine. Consequently, the photogenerated current density in the depletion region can be found by integrating the generation rate over the whole region

$$J_W = q \int_{y_j}^{y_j+W} G(y) dy = q\Phi_0 e^{-\alpha y_j} (1 - e^{-\alpha W}) \quad (9)$$

The total current must be constant throughout the device, and the different components remain constant along the depletion region. So, the total current can be calculated as sum of drift and diffusion currents in the edges of the depletion region:

$$J = J_W + J_n(y_j + W) + J_p(y_j) \quad (10)$$

The total current  $I$  is found by integrating the current density over the point source area,  $\Delta x \times \Delta z = \Omega$  ( $\Delta z = \Delta x$ )

$$I_I = \int_0^{\Delta z} \int_0^{\Delta x} J(y) dx dz = \Omega J \quad (11)$$

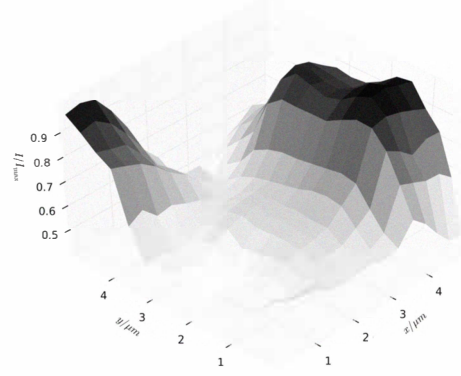


**Fig. 4.** Local relative photoresponse ( $I/I_{max}$ ) as a function of scan coordinates ( $x_s$ ,  $y_s$ ).

Regarding to the lateral depletion region illumination, (iii), the resulting total current  $I_{II}$  is calculated by integrating the generation rate over the aimed volume of the depletion region

$$I_{II} = q \int_0^{\Delta z} \int_0^{\Delta x} \int_0^{y_j+W} G(y) dy dx dz = q\Omega \Phi_0 (1 - e^{-\alpha(y_j+W)}) \quad (12)$$

Finally, the point source can aim at the surroundings of the photodiode (iv) at a point  $x = x'$ . The boundary condition at the point  $(x', y)$  is the result of solving the stationary continuity equation Eq. (1) under the boundary conditions  $n_p(y = 0) = n_p(\infty) = n_{p0}$ :

$$n_p(y) = n_{p0} + \frac{\Phi_0 \alpha \tau_n}{1 - \alpha^2 L_n^2} (e^{-\alpha y} - e^{-y/L_n}) \quad (13)$$

The minority carriers distribution in the surroundings of the photodiode is achieved solving the stationary continuity equation in  $x$  direction under following boundary conditions

$$D_n \frac{\partial^2 (n_p - n_{p0})}{\partial x^2} - \frac{n_p - n_{p0}}{\tau_n} = 0 \quad (14)$$

$$n_p(x_b) = n_{p0} e^{qV_{PD}/KT} \quad n_p(x') = n_p(y) \quad (15)$$

Therefore, the current density due to illumination in  $x'$  is  $J(x, y) = qD_n \frac{\partial n_p(x, y)}{\partial x}$  and the output current is the integral of the  $\Delta x$  contributions of the integral of the current density in the edge of the depletion region,  $x_b$ , over the lateral depletion region area

$$I_{III} = \int_{x_i}^{x_i+\Delta x} \left( \int_0^{\Delta z} \int_0^{y_j+W} J(x_b, y) dy dz \right) dx' \quad (16)$$

#### 4. RESULTS AND CONCLUSIONS

Pixels in a standard UMC 90nm technology were fabricated and measured under a point source illumination with

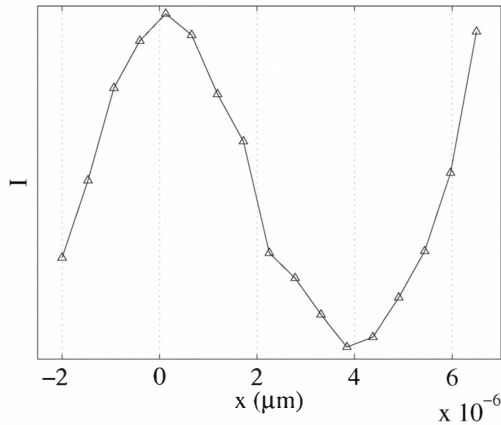


**Fig. 5.** Experimental results of the photoresponse of a p-N<sub>well</sub> junction ( $x_{\text{diff}} = 0.8\mu\text{m}$  and  $x_{\text{ph}} = 2.12\mu\text{m}$ ).

$\lambda=500\text{nm}$  and approximately  $0.5\mu\text{m}$  width to validate the accuracy of the proposed model. The pixels have a total area of  $4 \times 8\mu\text{m}^2$  divided into two equal parts of  $4 \times 4\mu\text{m}^2$ , one for the photodiode and the other one for the 3T-APS electronics. The photodiodes on the DUT are arranged together with the readout circuitry in a checkerboard-like matrix. For the electrical measurements of the local sensitivities all PD are connected in parallel and their terminal voltage as well as the supply and bias voltages of the DUT were kept at zero. The total generated photocurrent was measured directly with an electrometer.

Several measurements were carried out, e.g., with different sizes and junctions and various scanning resolutions. As an example, an area that includes a P-Nwell junction was scanned with a pretty high resolution (step size of  $330\text{nm}$ ) by moving the hexapod table with the attached DUT in the  $x_s y_s$  plane (Fig. 1) in both directions as depicted in Fig. 2. As a result, we obtained the relative photocurrent scan of an interesting region of the DUT, Fig. 4, where the dark and light areas represent the response of photodiode and electronics, respectively. Fig. 5 shows the current corresponding to a P-Nwell junction scanned at a step size of  $530\text{nm}$ . A different data set was chosen to make a comparison with the model because it includes one complete pixel, where the photodiode is centered in  $x=0$ , the electronics is from  $x=2\mu\text{m}$  to  $x=6\mu\text{m}$ ,  $x_{\text{diff}}=0.8\mu\text{m}$  and  $x_{\text{ph}}=2.12\mu\text{m}$ . As can be observed, the photoresponse of the electronics is not zero as it was supposed. This fact can represent effects such as dark current or crosstalk. The photodiode photoresponse given by the model for the same light source is depicted in Fig. 6, where only the photodiode region from  $x=-2\mu\text{m}$  to  $x=2\mu\text{m}$  is plotted for simplicity, and it shows close agreement with experimental data. In addition, the photoresponse for different values of wavelength is estimated (Fig. 6), revealing a relative increase of the lateral depletion region photoresponse for the shortest

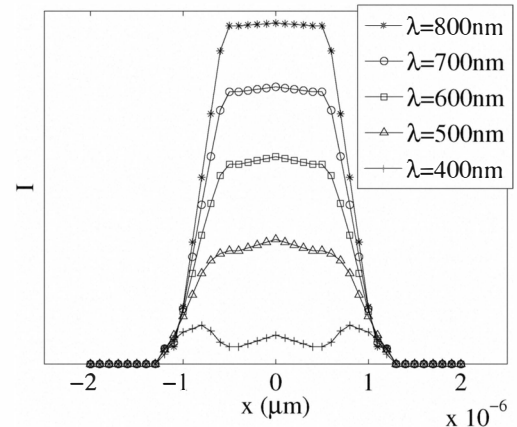


**Fig. 6.** Photoresponse of a p-N<sub>well</sub> junction given by the model ( $x_{\text{diff}} = 0.8\mu\text{m}$  and  $x_{\text{ph}} = 2.12\mu\text{m}$ ).

wavelength.

## 5. REFERENCES

- [1] ER Fossum, "CMOS image sensors: electronic camera-on-a-chip," *IEEE Trans. Electron Devices*, vol. 44, no. 10, pp. 1689–1698, 1997.
- [2] P.B. Catrysse and B.A. Wandell, "Roadmap for CMOS image sensors: Moore meets Planck and Sommerfeld," *Proc. SPIE*, vol. 5678, pp. 1–13, 2005.
- [3] H.S. Wong, "Technology and device scaling considerations for CMOS imagers," *IEEE Trans. Electron Devices*, vol. 43, no. 12, pp. 2131–2142, 1996.
- [4] H. Rhodes *et al.*, "CMOS imager technology shrinks and image performance," *2004 IEEE Workshop on Microelectronics and Electron Devices*, pp. 7–18, 2004.
- [5] I. Brouk and Y. Nemirowsky, "Dimensional effects in CMOS photodiodes," *Solid-State Electronics*, vol. 46, no. 1, pp. 19–28, 2002.
- [6] I. Shcherback, T. Danov, and O. Yadid-Pecht, "A comprehensive CMOS APS crosstalk study: photoresponse model, technology, and design trends," *IEEE Trans. Electron Devices*, vol. 51, no. 12, pp. 2033–2041, 2004.
- [7] B. Blanco-Filgueira *et al.*, "Bottom collection of photodiode-based CMOS APS," in *Int. Conf. on Advanced Semicond. Dev. and Microsyst.*, 2008, pp. 67–70.
- [8] L. Ravezzi *et al.*, "A versatile photodiode SPICE model for optical microsystem simulation," *Microelectronics Journal*, vol. 31, no. 4, pp. 277–282, 2000.